



Published in final edited form as:

Diabetologia. 2021 July ; 64(7): 1674–1689. doi:10.1007/s00125-021-05431-5.

Fasting and fasting mimicking treatment activate SIRT1/LXR α and alleviate diabetes-induced systemic and microvascular dysfunction

Sandra S. Hammer^{#1}, Cristiano P. Vieira^{#2}, Delaney McFarland¹, Maximilian Sandler¹, Yan Levitsky^{1,3}, Tim F. Dorweiler¹, Todd A. Lydic⁴, Bright Asare-Bediako², Yvonne Adu-Agyeiwaah², Micheli S. Sielski², Mariana Dupont², Ana Leda Longhini², Sergio Li Calzi², Dibyendu Chakraborty², Gail M. Seigel⁵, Denis A. Proshlyakov^{1,3}, Maria B. Grant^{#2}, Julia V. Busik^{#1}

¹Department of Physiology, Michigan State University, East Lansing, MI, USA

²Department of Ophthalmology and Visual Sciences, School of Medicine, The University of Alabama at Birmingham, Birmingham, AL, USA

³Department of Chemistry, Michigan State University, East Lansing, MI, USA

⁴Collaborative Mass Spectrometry Core, Michigan State University, East Lansing, MI, USA

⁵Center for Hearing and Deafness, University at Buffalo, Buffalo, NY, USA

These authors contributed equally to this work.

Abstract

Aims/hypothesis—*Homo Sapiens* evolved under conditions of intermittent food availability and prolonged fasting between meals. Periods of fasting are important for recovery from meal-induced oxidative and metabolic stress, and tissue repair. Constant high energy-density food availability in present-day society contributes to the pathogenesis of chronic diseases, including diabetes and its complications, with intermittent fasting (IF) and energy restriction shown to improve metabolic health. We have previously demonstrated that IF prevents the development of diabetic retinopathy in a mouse model of type 2 diabetes (*db/db*); however the mechanisms of fasting-induced health benefits and fasting-induced risks for individuals with diabetes remain largely unknown. Sirtuin 1 (SIRT1), a nutrient-sensing deacetylase, is downregulated in diabetes. In this study, the effect of SIRT1 stimulation by IF, fasting mimicking cell culture conditions

Corresponding author: Julia V. Busik, busik@msu.edu.

Contribution statement SSH and CPV were involved in conception and design of the study, acquisition, analysis and interpretation of data, and drafting and revising the manuscript, and gave final approval of the version to be published.

DM, MS, YL, TFD, TAL, BA-B, YA-A, MSS, MD, AL, SL, DC and GMS were involved in acquisition, analysis and interpretation of data and revising the manuscript, and gave final approval of the version to be published.

DAP, MBG and JVB were involved in conception and design of the study, analysis and interpretation of data, and drafting and revising the manuscript, and gave final approval of the version to be published.

JVB and MBG are the guarantors of the study and are responsible for the integrity of the work as a whole.

Publisher's Disclaimer: This Author Accepted Manuscript is a PDF file of a an unedited peer-reviewed manuscript that has been accepted for publication but has not been copyedited or corrected. The official version of record that is published in the journal is kept up to date and so may therefore differ from this version.

Authors' relationships and activities The authors declare that there are no relationships or activities that might bias, or be perceived to bias, their work.

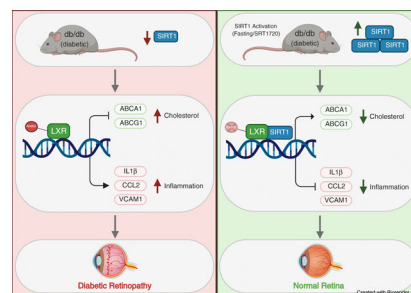
(FMC) or pharmacological treatment using SRT1720 was evaluated on systemic and retinal metabolism, systemic and retinal inflammation and vascular and bone marrow damage.

Methods—The effects of IF were modelled in vivo using *db/db* mice and in vitro using bovine retinal endothelial cells or rat retinal neuroglial/precursor R28 cell line serum starved for 24 h. mRNA expression was analysed by quantitative PCR (qPCR). SIRT1 activity was measured via histone deacetylase activity assay. NR1H3 (also known as Liver X receptor alpha (LXR α)) acetylation was measured via western blot analysis.

Results—IF increased *Sirt1* mRNA expression in mouse liver and retina when compared with non-fasted animals. IF also increased SIRT1 activity eightfold in mouse retina while FMC increased SIRT1 activity and expression in retinal endothelial cells when compared with control. *Sirt1* expression was also increased twofold in neuronal retina progenitor cells (R28) after FMC treatment. Moreover, FMC led to SIRT1-mediated LXR α deacetylation and subsequent 2.4-fold increase in activity, as measured by increased mRNA expression of the genes encoding ATP-binding cassette transporter (*AbcA1* and *AbcG1*). These changes were reduced when retinal endothelial cells expressing a constitutively acetylated LXR α mutant were tested. Increased SIRT1/LXR/ABC-mediated cholesterol export resulted in decreased retinal endothelial cell cholesterol levels. Direct activation of SIRT1 by SRT1720 in *db/db* mice led to a twofold reduction of diabetes-induced inflammation in the retina and improved diabetes-induced visual function impairment, as measured by electroretinogram and optokinetic response. In the bone marrow, there was prevention of diabetes-induced myeloidosis and decreased inflammatory cytokine expression.

Conclusions/interpretation—Taken together, activation of SIRT1 signalling by IF or through pharmacological activation represents an effective therapeutic strategy that provides a mechanistic link between the advantageous effects associated with fasting regimens and prevention of microvascular and bone marrow dysfunction in diabetes.

Graphical Abstract



Research in context

What is already known about this subject?

- Diabetes significantly reduces retinal sirtuin 1 (SIRT1)/liver X receptor α (LXR α) signalling
- Intermittent fasting prevents the development of diabetic retinopathy in a rodent model of type 2 diabetes
- SIRT1 is a nutrient-sensing deacetylase activated in low-nutrient environments

What is the key question?

- Can fasting or fasting mimicking pharmacological activation of SIRT1 be used as a strategy for prevention and treatment of diabetic retinopathy?

What are the new findings?

- Fasting and fasting mimicking conditions activate SIRT1/LXR α signalling in liver, bone marrow-derived cells, retina, retinal endothelial cells and neuronal retina progenitor cells
- Activation of SIRT1/LXR α by fasting mimicking conditions normalised cholesterol metabolism and prevented inflammation in retinal endothelial and neuronal cells
- Direct SIRT1 activation prevented diabetes-induced retinal inflammation and improved retinal function in type 2 diabetic mice

How might this impact on clinical practice in the foreseeable future?

- Direct activation of SIRT1 via pharmacological agents and/or intermittent fasting regimens could prove to be an effective therapeutic strategy to prevent microvascular and bone marrow dysfunction in diabetes.

Keywords

ABCA1; ABCG1; Cholesterol; Deacetylation; Diabetic retinopathy; Endothelial cell; Intermittent fasting; LXR; RPE; SIRT1

Introduction

In diabetes, the intricate balance between nutrient availability and utilisation is disturbed, leading to increased blood glucose levels, and dyslipidaemia characterised by increased plasma triacylglycerol and LDL-cholesterol levels and decreased HDL-cholesterol levels. High systemic nutrient availability is further exacerbated by the inability of tissues to access nutrients [1]. These changes result in macronutrient accumulation, proinflammatory and proapoptotic changes, and consequently vascular damage.

SIRT1, a member of the sirtuin family of NAD-dependent protein deacetylases, is a key metabolic regulator activated under low-nutrient states. Owing to the importance of SIRT1-mediated signalling in metabolism, deregulation of SIRT1 deacetylase activity results in chronic metabolic abnormalities. In diabetes, SIRT1 expression and activity are significantly decreased [2, 3], and activation of SIRT1 promotes insulin secretion, reduces insulin resistance and decreases body weight [4, 5]. Animal and in vitro studies have demonstrated the importance of SIRT1 regulation of inflammation [6, 7]. In the diabetic retina, increased DNA methylation of the SIRT1 promoter lead to transcriptional repression. Activation of SIRT1 is protective against diabetes-induced vascular and mitochondrial damage by inhibiting NF- κ B [8], poly [ADP-ribose] polymerase (PARP-1) [9] and matrix-metalloproteinase 9 (MMP-9) [2] activation and decreasing histone acetylation of the DNA (cytosine-5)-methyltransferase 1 (DNMT1) promoter [10]. Importantly, diabetes-induced decreases in SIRT1 signalling result in dysregulated cholesterol metabolism and increased production of proinflammatory cytokines via decreased liver X receptor (LXR) signalling [11]. SIRT1 is critical to vascular health [12, 13]. SIRT1 levels fall with the development of macrovascular disease while maintaining SIRT1 levels prevents macrovascular damage [14]. Similarly, decreased SIRT1 levels have been implicated in the pathogenesis of microvascular complications [2].

Diabetic retinopathy is the most common microvascular complication [15], where high metabolic demands of the retina dictate complex regulatory pathways needed to meet retinal energy needs while preserving the delicate balance between nutrient availability and tightly regulated retinal lipid metabolism [16]. Normally, the retina maintains its cholesterol homeostasis by a tight control of cholesterol input/output [17]. Under normal conditions, cholesterol input in the retina includes local biosynthesis [18] [19] and uptake of the lipoprotein particles from the circulation [20–22] on the basal membrane of retinal pigment epithelium (RPE) cells.

Intermittent fasting (IF) was recently shown to have multiple health benefits and is now pursued as a metabolic strategy for management of obesity and other metabolic diseases, including diabetes. IF is not without considerable risks for individuals with diabetes [23–25]. There is insufficient clinical data regarding the safety of IF for diabetic patients; therefore

having a pharmacological regimen that mimics fasting may have major clinical relevance. Fasting regimens and SIRT1 activation have been shown to increase longevity and delay onset of disease in yeast, fruit flies, mice and more recently, non-human primate animal models [26]. Fasting-induced SIRT1 activation has been linked to increased NAD⁺ levels, increased mitochondrial biogenesis and delayed senescence [27, 28]. The current study addresses the use of fasting and fasting mimicking treatments to activate SIRT1 signalling.

Methods

Animal studies

All animal procedures were in compliance with the NIH *Guide for the care and use of laboratory animals*, and with the Association for Research in Vision and Ophthalmology *Statement for the use of animals in ophthalmic and vision research* (IACUC #10917). For *db/db* mouse (strain B6.BKS(D)-*Lepr*^{db}/J [stock #000697] purchased from Jackson Laboratory, USA) studies, male mice were treated with 100mg/kg body weight/day SRT1720 in their chow for 6 months after diabetes onset around 10 weeks of age [29]. Mice were considered diabetic after two consecutive daily measurements of blood glucose levels of 13.9 mmol/l or higher. *db/db* and *db/m* mice without treatment were analysed as control animals.

Cell culture and treatment

Bovine retinal endothelial cells (BRECs) were isolated from mycoplasma-free bovine tissue and validated according to a previously published protocol [11, 30]. BREC identity was authenticated morphologically and using anti-von Willebrand factor immunocytochemistry (Abcam; UK; ab6994, RRID:AB305689) and LDL uptake assay (Abcam; ab133127) [31]. All antibodies used in this study were diluted based on the manufactures guidelines. BRECs were cultured in 10% FBS BREC complete media with 1% antibiotic/antimycotic (AA) (ThermoFisher; USA; 15240062) [32, 33]. MCDB131 media was used to make BREC complete media (Sigma; USA; m8537) using mycoplasma-free reagents. Passages 4–8 were used for all experiments. In order to model a fasting environment in vitro, BRECs were cultured in 0% FBS for 24h (fasting mimicking cell culture conditions [FMC]). FMC media contained endothelial growth factors and 5 mmol/l glucose [32]. Base media only contained MCDB131 media (m8537). Cells were treated with 1 µg/ml *N,N*-dimethyl-3β-hydroxy-cholenamide (DMHCA; Avanti Polar Lipids; USA; 700125), 1µg/ml SRT1720 (Selleckchem; USA; S1129) or 10ng/ml diabetic relevant stimuli TNF-α (R&D Systems; USA; 210-TA020), for 24h. Cells were transfected using either *Sirt1* siRNA or scrambled *Sirt1* siRNA as control (Invitrogen; USA; 81801753) for 24h with the Human Coronary Artery Endothelial Cell Nucleofactor kit (Lonza; Switzerland; VPB-1001, S005). CBA-hLXR-alpha-q43 AAV2 vectors were custom made in the Department of Ophthalmology at the University of Florida, USA; referred to as Q432 throughout. The heterogeneous adherent rat retinal neuroglial/precursor R28 cell line was acquired from G. M. Seigel at the University at Buffalo, USA. R28 cells were cultured in DMEM+ media with 10% calf serum. Cells were treated with FMC for 24h. Cells used for all cell culture experiments were selected at random from different isolations. Experimental analysis was not conducted in a blinded matter.

Cell death assays

BRECs were cultured in FMC or basal media for 24–96h. Basal media was comprised of only MCB131 media without the addition of growth factors or supplements (m8537). This media was used as a positive control for cell death. Cell death was analysed via Trypan Blue exclusion assay [34] and annexin V (Abcam; ab14085). Cell death was calculated by dividing the number of dead cells by the total number of cells or by measuring intensity density of annexin V + cells, for Trypan Blue or annexin V assays, respectively. Apoptosis was thermally induced (50°C for 10min) as a positive control.

qPCR

RNA was isolated using RNeasy mini kit (Qiagen; USA; 74106) according to the manufacturer's instructions. Gene-specific forward and reverse primers (Integrated DNA Technologies; USA) are shown in ESM Table 1 and were subjected to real-time quantitative PCR (qPCR) quantification using the ABI PRISM 7700 Sequence Detection System (Applied Biosystems; USA). Inflammatory primers were chosen based on relevance to cell type. For whole retina, the macrophage and microglia contribution to the inflammatory phenotype makes IL-1 β and CCL2 the relevant markers to investigate [35]. For endothelial cells, contribution of IL-1 β and C-C motif chemokine ligand 2 (CCL2) to inflammation is minimal when compared with vascular cell adhesion protein 1 (VCAM1) [36, 37]. All reactions were performed in duplicate from at least three independent biological samples. Cyclophilin A was used as a control, and results were analysed using the comparative C_t method and C_t values were normalised to cyclophilin A levels. Data are shown as normalised relative to control levels or as non-normalised raw expression levels.

Western blot and immunoprecipitation

BRECs were cultured and treated as above. Lysates were processed as previously described [11]. To determine active LXRA levels, two identical aliquots of the cell lysate samples corresponding to 50 μ g of total protein were used for western blot detection using LXRA (Abcam; ab3585, RRID:AB_303930), and β -actin antibodies (Cell Signalling Technology; USA; Cat# 4970, RRID:AB_2223172); and for acetylation studies using LXRA antibody for immunoprecipitation (LSBio, USA; LS-C374316), and acetylated lysine #9441 (Cell Signalling Technology; RRID:AB_331805) antibody for immunoblotting. Complete immunoprecipitation was verified by the absence of LXR signal in the post-immunoprecipitation sample. Active LXR was calculated by subtracting acetylated LXR signal from total LXR signal in each sample. Total acetylated lysine was assayed using the immunoprecipitation kit Dynabeads Protein A (Invitrogen; 10006D). Blocking buffer for fluorescent western blotting MB-070 (Rockland; USA) was used for dilution of the antibodies. Dilution for secondary antibody was 1:1000. Blots were analysed using the LICOR Odyssey (LICOR Biosciences; USA) imaging and quantification system.

HDAC assay

SIRT1 activity was measured using the histone deacetylase (HDAC) Kit (ABCAM; ab156064) according to the manufacturer's instructions. Results are shown as fluorescence

measurements at 355nm and 460nm excitation and emission, respectively over total protein. Samples were normalised to control.

Mitochondrial respiration measurements

Respiration of BRECs was measured using a microrespirometer as previously described [38]. Briefly, On the day of measurements, the chips were closed, mounted in a microrespirometer, and immediately perfused at a constant $10\mu\text{l min}^{-1}$ flow rate. Perfusion was controlled by a Harvard Apparatus syringe infusion pump. Cells were first perfused with 10% FBS media for 12 h, followed by perfusion with serum-free media for an additional 24 h. Respiratory activity was measured for 15 min in stationary medium, with a minimum of 15 min of re-perfusion between measurements. Total oxygen concentration was maintained above $200\mu\text{mol/l}$ in all cases. Measurements in the presence of potassium cyanide ($\text{KCN}, 5\mu\text{mol l}^{-1}$) were used to correct for non-mitochondrial oxygen consumption. Respiratory activity was calculated by linear fitting of the initial 5 min of steady oxygen consumption. The instrument was calibrated using air-equilibrated media as an aerobic standard and 1 mmol l^{-1} sodium dithionite in media as anaerobic standard.

Cholesterol measurement

In vivo—For lipid extraction, lipids from mouse retinas were extracted with methanol, chloroform, and water as previously described [39, 40].

For the analysis of free and total sterol content, sterols were analysed by high resolution/accurate mass LC-MS/MS using a Thermo Scientific LTQ-Orbitrap Velos LC-MS system as previously described [41]. Cholesterol identification was performed by comparison of retention time, exact mass, and MS/MS profile to an authentic standard purchased from Steraloids.

In vitro—Total cholesterol levels were measured using the Amplex Red Cholesterol Assay kit (Thermo Scientific; A12216) according to the manufacturer's instructions. Briefly, cells were diluted in $1\times$ reaction buffer and incubated with a working solution containing $300\mu\text{mol/l}$ Amplex Red reagent. Fluorescence was measured at 590 nmol/l after 45 min at 37°C .

Immunohistochemical staining

Retinas were processed as previously described [42] using the following antibodies: primary monoclonal antibody for CD45 (R&D Systems; MAB114, RRID:AB_357485) with secondary Alexa Fluor 594 (A11007, Invitrogen, USA); primary ionised calcium binding adaptor molecule 1 (Iba-1; Fujifilm Cellular Dynamics; USA; 019–19741, RRID:AB_839504) with secondary Alexa Fluor 488 (A27023, Invitrogen USA) and NeuN (Millipore Sigma, USA; clone A60, Alexa Fluor 488 conjugated MAB377X) at 1:50; 1:500 and 1:100 dilutions, respectively. The antibodies were diluted in PBS with 1% normal goat serum (G9023 Sigma Aldrich, USA). Dilution for the secondary antibodies was 1:1000. The images were analysed in blinded manner.

Visual function studies

ERG studies—Electroretinogram (ERG) studies were performed as previously described with assessment of photopic and scotopic responses using UTAS Bigshot (LKC Technologies, USA) [43].

Optomotor response—The visual acuity of the mice was determined by use of optomotor response recordings using OptoMotry 1.7.7 (Cerebral Mechanics, Canada) [44, 45].

Statistical analyses

A Student's two tailed *t* test was used for comparisons between two groups. One-way ANOVA, followed by the Tukey post hoc test, was used for multiple comparisons. All values are expressed as mean \pm SEM. A value of $p < 0.05$ was considered to be statistically significant. Statistical tests were performed using statistics software (GraphPad Software, USA).

Results

Fasting increases SIRT1 expression and activity

We determined the effect of IF for 48h on SIRT1 expression and activity in control mice. *Sirt1* mRNA expression was significantly higher in the liver (Fig. 1a) with a tendency towards higher retinal *Sirt1* expression (Fig. 1b) and eightfold increase in activity (Fig. 1c) in fasting animals compared with control non-fasting animals.

Fasting mimicking conditions activate SIRT1/LXR signalling in retinal vascular cells and neuronal cells

We next performed studies using BRECs and neuronal cell culture (R28) models. FMC (0% FBS) was used to model the low-nutrient, energy-reduced state of IF. FMC was also effective in activating SIRT1 HDAC and expression twofold in BRECs (Fig. 2a, b). Consequently, increased deacetylase activity resulted in 2.4-fold increased LXR α activity, as measured by expression of reverse cholesterol export (RCT) genes, ATP-binding cassette transporter A1 and G1 (*Abca1* and *Abcg1*, respectively) (Fig. 2c). Treatment with FMC also decreased VCAM1 in BRECs (Fig. 2d).

In order to assess the effect of FMC-induced SIRT1 activation in neuronal cells, SIRT1/LXR α activity was measured in R28 cells. Treatment with FMC significantly increased *Sirt1* and *Lxra* expression and increased LXR α activity, as measured by ABCA1 expression (Fig. 2e).

Active and total LXR α protein levels were significantly increased in BRECs treated with FMC (Fig. 3a–d). To determine if LXR α activation and control of cholesterol metabolism is through the direct deacetylation of LXR α by SIRT1, we used a constitutively acetylated lysine–glutamine K432Q LXR α mutant (Q432). BRECs infected with this mutant had a blunted response to SIRT1 activation by SRT1720 as determined by LXR α expression (Fig. 3e) and LXR α activity measured by *Abca1* expression (Fig. 3f).

As shown in Fig. 4a, BRECs were treated with TNF- α to recapitulate the diabetic milieu and this resulted in increased cholesterol levels. By contrast, FMC prevented TNF- α -induced cholesterol accumulation in BRECs (Fig. 4a). As expected, activation of LXR α via DMHCA, a steroidal LXR ligand, significantly reduced BREC cholesterol levels. Treatment with FMC, in combination with DMHCA administration, significantly augmented cholesterol export and lowered BREC cholesterol levels even further when compared with DMHCA treatment alone (Fig. 4b).

In addition to augmenting cholesterol export, FMC in BRECs prevented the upregulation of the NF- κ B-dependent proinflammatory gene, *Vcam1* (Figure 2d). Importantly, data shown in Fig. 4c highlights the importance of SIRT1 signalling in regulating the FMC-induction of RCT and the anti-inflammatory responses in BRECs. Loss of SIRT1, via SIRT1-directed siRNA, prevents FMC-induced upregulation of ABCA1, ABCG1 and downregulation of VCAM1 (Fig. 4c).

Cell death and mitochondrial respiration are not affected by FMC

To ensure the safety of FMC, cell death and mitochondrial respiration were measured after 24h in FMC-treated BRECs. As shown in Fig. 5a, b and c, cell death, measured by Trypan Blue exclusion assay and annexin V, did not significantly differ between FMC-treated cells and BRECs cultured in control conditions (10% FBS-containing medium). The primary goal of these experiments was to assess the effect of serum starvation on SIRT1/LXR α , and so the FMC treatment media contains growth factors and 5 mmol/l glucose, and the only component that is missing from this media is FBS. Notably, cells treated with basal media, without growth factors, glucose, or FBS, have increased cell death when compared with control or cells treated with FMC media (ESM Fig. 1). Moreover, there is no statistical difference between mitochondrial respiration in cells cultured in FMC or control conditions: FMC respiratory activity was $0.0555 \pm 0.0058 \mu\text{mol l}^{-1} \text{s}^{-1}$ compared with $0.0507 \pm 0.005 \mu\text{mol l}^{-1} \text{s}^{-1}$ in control (Fig. 5d).

Diabetes-induced retinal cholesterol accumulation and inflammation are prevented by SIRT1 activation

In order to investigate the effect of SIRT1 activation on diabetic retinopathy progression, control and *db/db* animals were fed chow containing the SIRT1 activator, SRT1720 for 6 months following the onset of diabetes. Diabetes significantly reduced SIRT1 retinal expression. Treatment of diabetic animals with SRT1720-containing chow significantly increased SIRT1 expression compared with retinas from diabetic mice fed control chow (Fig. 6a,b).

As expected, diabetes resulted in elevated retinal cholesterol levels when compared with control retinas. Treatment with SRT1720 reduced diabetes-induced inflammation twofold, as measured by expression of *Il-1 β* and *Ccl-2* (Fig. 6c), as well as a reduction in the number of Iba-1⁺ and CD45⁺ cells in the retina (Fig. 6e-h). SIRT1 activation, via SRT1720, also restored cholesterol levels in diabetic retinas to non-diabetic levels (Fig. 6d). As shown in Fig. 6i-l, the development of acellular capillaries was significantly increased in *db/db* mice

(red arrows) while activation of SIRT1, via SRT1720 treatment, restored the number of acellular capillaries to non-diabetic levels.

The anti-inflammatory effect of SRT1720 treatment extended to the diabetic bone marrow. Typically, in chronic diabetes the bone marrow supernatant has elevated proinflammatory cytokines, which serve to skew haematopoiesis towards generation of increased myeloid cells [46]. SRT1720 treatment resulted in a reduction in the expression of the inflammatory cytokines *Tnf- α* and *Ccl-2* in the bone marrow supernatant (Fig. 7a, b). The colony-forming capability of bone marrow-derived (BMD) cells from the SRT1720-treated diabetic cohort showed an increase in megakaryocyte–erythroid progenitors (MEPs) (Fig. 7c) compared with untreated diabetic animals. These findings in the bone marrow are similar to what we observed when *db/db* mice were treated with the LXR α agonist DMHCA [47]. Bone marrow circulating angiogenic cells (CACs) showed the typical reduction in the 6 month *db/db* mice compared with controls (Fig. 7d). Further examination of myeloid lineage in the bone marrow showed that there were no changes in common myeloid progenitors (CMP, ESM Fig. 2a) and an increase in granulocyte-macrophage progenitors (GMP, ESM Fig. 2b) in diabetes. SRT1720 treatment did not affect CMP and GMP levels (ESM Fig. 2a, b). Examination of the peripheral blood from the experimental cohorts demonstrated that diabetes resulted in the reduction of CACs in the peripheral blood but there was no increase in CACs in SRT1720-treated mice (Fig. 7e). *db/db* mice showed the typical increase in total circulating monocytes (Fig. 7f) with a decrease in classical (ESM Fig. 2c) and an increase in non-classical monocytes (ESM Fig. 2d) but no changes were observed in the SRT1720-treated diabetic mice. While systemic effects of SRT1720 were not readily apparent from changes in peripheral blood cells, in vitro studies of BMD macrophages were highly informative (Fig. 7g, h). When BMD macrophages from diabetic and control mice were polarised to M2 macrophages, a diabetes-induced decrease in the expression of *Lxra* and the LXR-controlled target genes, *Abca1* and *Abcg1* was observed compared with controls. SRT1720 increased SIRT1 expression in M2 macrophages from diabetic mice leading to upregulation of LXR α activity as shown by an increase in *Abcg1* expression (Fig. 7h).

SIRT1 activation prevents retinal vascular and neurodegeneration in vivo

Neuronal damage and loss (Fig. 8a) precede the microangiopathy of diabetic retinopathy. As expected, diabetes resulted in a loss of neurons as measured by NeuN⁺ immunohistochemistry (Fig. 8b). Administration of SRT1720 significantly preserved NeuN⁺ expression, predominately localised in the retinal ganglion cell layer (Fig. 8b).

SIRT1 activation improves visual function in *db/db* mice

The functional effect of SIRT1 activation in diabetes was assayed by measuring retinal and visual function of *db/db* mice fed control or SRT1720-containing chow. As expected, ERG of *db/db* mice showed decreased amplitude of scotopic a- and b-waves and lower photopic b-waves. ERG responses were restored to non-diabetic levels in SRT1720-treated diabetic mice (Fig. 8c,d). Visual response assayed using optokinetic (OKN) response measurements was significantly lower in diabetic mice when compared with control mice and SIRT1 activation similarly restored visual acuity to control levels (Fig. 8e).

Discussion

The beneficial effects of fasting in improving metabolic health, warding off chronic disease and increasing longevity have been established by several well-designed clinical trials; however, the data on IF in diabetic individuals remain limited [48, 49] and potential risks associated with IF in people with diabetes have to be carefully considered before it can become a viable treatment option. These include the risk of hypoglycaemia in patients on glucose-lowering medications (insulin, sulfonylureas) [24], and increased glucose level fluctuations between the feeding and fasting days [48].

This study provides one of the first mechanistic evaluations of the effect of SIRT1 activation by fasting, FMC or pharmacological approaches in the diabetic retina. Regulation of SIRT1 by nutrient availability in the liver is well known, however retinal SIRT1 regulation is less well understood, in part, due to the complex multicellular nature of the retina. As shown in this study, fasting-induced upregulation of SIRT1 was not evident in the whole retina, but was uncovered when cell-specific studies using BRECs and neuronal cells were performed. Importantly, the role of SIRT1 activation in normalising cholesterol metabolism in the diabetic retina and in bone marrow cells is demonstrated in this study. In health, the bone marrow has a perfect balance of immunomodulatory cells and vascular reparative populations. This balance is disturbed in chronic diabetes and can contribute to microvascular dysfunction as is seen in diabetic retinopathy [50–52]. In this study, we see a tendency toward improvement in the vascular reparative population, called circulating angiogenic cells (CACs). Cholesterol accumulation adversely impacts this population [53], which is exquisitely sensitive to the diabetic milieu [54]. High glucose adversely influences CAC function by reducing SIRT1/LXR [55, 56], while increasing SIRT1/LXR in CACs of diabetic origin corrects their dysfunction [57]. Systemic dyslipidaemia also impacts circulating monocytes to promote their activation to a highly proinflammatory state [58], which causes retinal damage. Thus, systemic and retinal SIRT1/LXR-mediated metabolic abnormalities simultaneously reduce vascular repair and also promote vascular damage by increasing inflammation.

Bone marrow pathology in the advanced stages also includes reduced erythropoiesis [59]. SRT1720 exhibited anti-inflammatory effects on the bone marrow supernatant and simultaneously increased the generation of megakaryocytes and erythrocytes. These findings suggest that SRT1720 has potential beneficial effects beyond the retina.

Using novel tools to examine long-term monitoring of mitochondrial function in BRECs, we demonstrated that, while providing the beneficial metabolic effects, FMC is devoid of detrimental effects on mitochondrial respiration and energy production. In addition to well described vascular effects, this study demonstrated the role of fasting-induced SIRT1 activation in the improvement of diabetes-induced neuronal damage, both in vivo and in vitro.

SRT1720 has been previously shown to increase lifespan and improve overall health in mice fed a high-fat diet as well as those fed a normal diet [60, 61]. Activation of SIRT1, via SRT1720, has been shown to significantly improve insulin sensitivity, lower glucose levels

and increase mitochondrial and metabolic function [62]. SRT1720 was shown to activate SIRT1 with potencies 1,000-fold greater than resveratrol, another SIRT1 activator. Although administration of SRT1720 was successful in activating retinal SIRT1 levels in our studies and in diabetic individuals, not all studies support efficacy [63]

Moreover, there is contradictory evidence as to the pro-survival properties of SIRT1 activation. Zarse et al demonstrated the negative effects that SRT1720 has on *C. elegans* lifespan [64]. These confounding effects could be due to the governing role that SIRT1 plays in regulating circadian rhythm in peripheral tissues. Several studies have demonstrated SIRT1 activation of *Bmal1* (also known as *Arntl*) and *Clock* genes, resulting in robust circadian restoration [65]. Thus, differences in timing and feeding patterns among different studies could result in varied physiological outcomes.

In addition to pharmacological activation of SIRT1, we show that FMC activates SIRT1/LXR α signalling in BRECs and neuronal cells (Fig. 2). Numerous studies highlight the beneficial effects IF and energy-restriction regimens on preventing diabetes-associated complications [42, 66, 67]. Recently, the beneficial effects of energy restriction were demonstrated by a clinical trial in which participants who maintained reduced energy intake for 2 years had a significant reduction in heart disease and diabetes prevalence [68]. The mechanism of action responsible for these beneficial effects, however, is still under active investigation.

High demand for cholesterol in the retina dictates its unique metabolism with local retinal cholesterol production coupled with import from the circulation. Under healthy conditions, cholesterol enters the retina via the outer blood–retinal barrier through LDL receptor-mediated processes. Rapid cholesterol turnover in the retina requires efficient cholesterol export. Retinal cells express several hydroxylases (CYP27A1, CYP46A1, CYP11A1) that metabolise cholesterol to more soluble oxysterols [35]. Unlike cholesterol, oxysterols can rapidly diffuse out of the retina for the delivery to the liver for generation of bile acids. Additionally, oxysterols produced by CYP27A1 and CYP46A1 activate LXR α , promoting LXR α -mediated retinal cholesterol export through activation of the RCT pathway via increased ABCA1 and ABCG1 expression in both inner (REC) and outer (RPE) retinal barrier. In the diabetic environment, both cholesterol uptake and removal from the retina are affected, resulting in elevated and dysregulated retinal cholesterol levels. The leaky retinal endothelial cells lead to increased cholesterol ingress, and the decrease in oxysterol levels and LXR activity result in cholesterol accumulation in the retina. In addition to the increase in RCT, activation of LXR α results in repression of NF- κ B dependent proinflammatory gene upregulation in the retinal cells.

SIRT1 mediates a decrease in histone acetylation of the DNMT1 promoter. Interestingly, a feedback regulation of SIRT1 expression by DNMT1 through increased DNA methylation of the SIRT1 promoter resulting in SIRT1 transcriptional repression was demonstrated in the diabetic retina [10]. Figure 6 demonstrates the detrimental effects that type 2 diabetes has on retinal SIRT1 expression, cholesterol metabolism and inflammation. In diabetic mice, activation of SIRT1 via SRT1720 restores SIRT1 expression and cholesterol levels to normal. Additionally, diabetes-induced retinal inflammation is significantly reduced after

SRT1720 treatment. It is important to note that SRT1720's ability to increase SIRT1 expression in vitro and in vivo suggests a potential novel mechanism of action unique to the retina and retinal cells since other studies done in non-retinal tissues have not shown increases in SIRT1 expression after SRT1720 treatment [61]. Additionally, activation of SIRT1 has beneficial physiological effects as seen by the prevention of diabetic retinopathy-induced acellular capillary formation, a hallmark of diabetic retinopathy progression. Notably, in vivo activation of SIRT1 restores visual function in *db/db* mice as measured by ERG and OKN response.

In summary, this study examined the impact of the excess energy supply of type 2 diabetes on downregulation of SIRT1. Decreased LXR α signalling, a hallmark feature of type 2 diabetes, leads to dysregulated retinal cholesterol metabolism and increased production of proinflammatory cytokines. SIRT1 action, however, is not limited to LXR α signalling as activation of SIRT1 in the diabetic retina was protective against inflammation and mitochondrial damage by deacetylation and inhibition of NF- κ B, PARP-1 and MMP-9 signalling [8, 9, 69]. Activation of SIRT1 supports normal mitochondrial respiration and energy production under FMC conditions without cell death and mitochondrial damage. Importantly, this study supports the growing evidence for the effective and advantageous effects of modulating time and quantity of nutrient intake and the need to expand strategies for individuals with diabetes that are safe and devoid of hypoglycaemic complications but remain metabolically robust.

Supplementary Material

Refer to Web version on PubMed Central for supplementary material.

Acknowledgements

M. Gorbatyuk and T. W. Kraft (School of Optometry, University of Alabama at Birmingham, USA) provided UTAS Bigshot (LKC Technologies, USA) for ERG studies, and OptoMotry 1.7.7 (Cerebral Mechanics, Canada) for the visual acuity studies.

Funding

This study was supported by the National Institutes of Health Grants R01EY012601, R01EY028858, R01EY028037, R01EY025383 to MBG; T32HL134640-01 to MD; F32EY028426 to SSH; MICL02539, R01EY030766, R01EY016077 to JVB, R01EY028049 to DAP; NIH-5-R25-HL108864 to MS.

Data availability

The authors confirm that the data supporting the findings of this study are available within the article and its supplementary materials.

Abbreviations

ABCA1	ATP-binding cassette transporter A1
ABCG1	ATP-binding cassette transporter G1
BMD	Bone marrow-derived

BREC	Bovine retinal endothelial cell
CAC	Circulating angiogenic cell
CCL2	C-C motif chemokine ligand 2
CMP	Common myeloid progenitors
DMHCA	<i>N,N</i> -dimethyl-3 β -hydroxy-cholenamide
DNMT1	DNA (cytosine-5)-methyltransferase 1
ERG	Electroretinogram
FMC	Fasting mimicking cell culture conditions
GMP	Granulocyte-macrophage progenitors
HDAC	Histone deacetylase
Iba-1	Ionised calcium binding adaptor molecule 1
IF	Intermittent fasting
LXR	Liver X receptor
MEP	Megakaryocyte–erythroid progenitor
MMP-9	Matrix-metallopeptidase 9
OKN	Optokinetic
PARP-1	poly [ADP-ribose] polymerase
qPCR	Quantitative PCR
RCT	Reverse cholesterol transport
RPE	Retinal pigment epithelium
SIRT1	Sirtuin 1
VCAM1	Vascular cell adhesion protein 1

References

- [1]. Eshaq RS, Aldalati AMZ, Alexander JS, Harris NR (2017) Diabetic retinopathy: Breaking the barrier. *Pathophysiology* 24(4): 229–241. 10.1016/j.pathophys.2017.07.001 [PubMed: 28732591]
- [2]. Kowluru RA, Santos JM, Zhong Q (2014) Sirt1, a negative regulator of matrix metalloproteinase-9 in diabetic retinopathy. *Invest Ophthalmol Vis Sci* 55(9): 5653–5660. 10.1167/iovs.14-14383 [PubMed: 24894401]
- [3]. Karbasforooshan H, Karimi G (2018) The role of SIRT1 in diabetic retinopathy. *Biomed Pharmacother* 97: 190–194. 10.1016/j.biopha.2017.10.075 [PubMed: 29091865]
- [4]. Wang RH, Kim HS, Xiao C, Xu X, Gavrilova O, Deng CX (2011) Hepatic Sirt1 deficiency in mice impairs mTorc2/Akt signaling and results in hyperglycemia, oxidative damage, and insulin

- resistance. *The Journal of clinical investigation* 121(11): 4477–4490. 10.1172/JCI46243 [PubMed: 21965330]
- [5]. Baur JA, Pearson KJ, Price NL, et al. (2006) Resveratrol improves health and survival of mice on a high-calorie diet. *Nature* 444(7117): 337–342. 10.1038/nature05354 [PubMed: 17086191]
- [6]. Yun JM, Chien A, Jialal I, Devaraj S (2012) Resveratrol up-regulates SIRT1 and inhibits cellular oxidative stress in the diabetic milieu: mechanistic insights. *The Journal of nutritional biochemistry* 23(7): 699–705. 10.1016/j.jnutbio.2011.03.012 [PubMed: 21813271]
- [7]. Zabolotny JM, Kim YB (2007) Silencing insulin resistance through SIRT1. *Cell metabolism* 6(4): 247–249. 10.1016/j.cmet.2007.09.004 [PubMed: 17908551]
- [8]. Kowluru RA, Mishra M, Kumar B (2016) Diabetic retinopathy and transcriptional regulation of a small molecular weight G-Protein, Rac1. *Exp Eye Res* 147: 72–77. 10.1016/j.exer.2016.04.014 [PubMed: 27109029]
- [9]. Mishra M, Kowluru RA (2017) Role of PARP-1 as a novel transcriptional regulator of MMP-9 in diabetic retinopathy. *Biochim Biophys Acta Mol Basis Dis* 1863(7): 1761–1769. 10.1016/j.bbadis.2017.04.024 [PubMed: 28478229]
- [10]. Mishra M, Duraisamy AJ, Kowluru RA (2018) Sirt1: A Guardian of the Development of Diabetic Retinopathy. *Diabetes* 67(4): 745–754. 10.2337/db17-0996 [PubMed: 29311218]
- [11]. Hammer SS, Beli E, Kady N, et al. (2017) The Mechanism of Diabetic Retinopathy Pathogenesis Unifying Key Lipid Regulators, Sirtuin 1 and Liver X Receptor. *EBioMedicine* 22: 181–190. 10.1016/j.ebiom.2017.07.008 [PubMed: 28774737]
- [12]. Mattagajasingh I, Kim CS, Naqvi A, et al. (2007) SIRT1 promotes endothelium-dependent vascular relaxation by activating endothelial nitric oxide synthase. *Proceedings of the National Academy of Sciences of the United States of America* 104(37): 14855–14860. 10.1073/pnas.0704329104 [PubMed: 17785417]
- [13]. Potente M, Dimmeler S (2008) Emerging roles of SIRT1 in vascular endothelial homeostasis. *Cell Cycle* 7(14): 2117–2122 [PubMed: 18641460]
- [14]. Miranda MX, van Tits LJ, Lohmann C, et al. (2014) The Sirt1 activator SRT3025 provides atheroprotection in Apoe^{-/-} mice by reducing hepatic Pcsk9 secretion and enhancing Ldlr expression. *European heart journal*. 10.1093/eurheartj/ehu095
- [15]. Centers for Disease Control and Prevention (2020) National Diabetes Statistics Report. Available from: <https://www.cdc.gov/diabetes/data/statistics-report/index.html>. Accessed Sep 2020
- [16]. Chang YC, Wu WC (2013) Dyslipidemia and diabetic retinopathy. *Rev Diabet Stud* 10(2–3): 121–132. 10.1900/RDS.2013.10.121 [PubMed: 24380088]
- [17]. Fliesler SJ, Bretillon L (2010) The ins and outs of cholesterol in the vertebrate retina. *J Lipid Res* 51(12): 3399–3413. jlr.R010538 [pii] 10.1194/jlr.R010538 [PubMed: 20861164]
- [18]. Lin JB, Mast N, Bederman IR, et al. (2016) Cholesterol in mouse retina originates primarily from *in situ* de novo biosynthesis. *J Lipid Res* 57(2): 258–264. 10.1194/jlr.M064469 [PubMed: 26630912]
- [19]. Zheng W, Reem RE, Omarova S, et al. (2012) Spatial distribution of the pathways of cholesterol homeostasis in human retina. *PLoS One* 7(5): e37926. 10.1371/journal.pone.0037926 [PubMed: 22629470]
- [20]. Pikuleva IA, Curcio CA (2014) Cholesterol in the retina: the best is yet to come. *Prog Retin Eye Res* 41: 64–89. 10.1016/j.preteyeres.2014.03.002 [PubMed: 24704580]
- [21]. Tserentsoodol N, Sztejn J, Campos M, et al. (2006) Uptake of cholesterol by the retina occurs primarily via a low density lipoprotein receptor-mediated process. *Molecular vision* 12: 1306–1318 [PubMed: 17110914]
- [22]. Duncan KG, Hosseini K, Bailey KR, et al. (2009) Expression of reverse cholesterol transport proteins ATP-binding cassette A1 (ABCA1) and scavenger receptor BI (SR-BI) in the retina and retinal pigment epithelium. *The British journal of ophthalmology* 93(8): 1116–1120 [PubMed: 19304587]
- [23]. Carter S, Clifton PM, Keogh JB (2018) Effect of Intermittent Compared With Continuous Energy Restricted Diet on Glycemic Control in Patients With Type 2 Diabetes: A Randomized Noninferiority Trial. *JAMA Netw Open* 1(3): e180756. 10.1001/jamanetworkopen.2018.0756 [PubMed: 30646030]

- [24]. Grajower MM, Horne BD (2019) Clinical Management of Intermittent Fasting in Patients with Diabetes Mellitus. *Nutrients* 11(4). 10.3390/nu11040873
- [25]. Harris L, Hamilton S, Azevedo LB, et al. (2018) Intermittent fasting interventions for treatment of overweight and obesity in adults: a systematic review and meta-analysis. *JBI Database System Rev Implement Rep* 16(2): 507–547. 10.11124/JBISRIR-2016-003248
- [26]. Yuan Y, Cruzat VF, Newsholme P, Cheng J, Chen Y, Lu Y (2016) Regulation of SIRT1 in aging: Roles in mitochondrial function and biogenesis. *Mech Ageing Dev* 155: 10–21. 10.1016/j.mad.2016.02.003 [PubMed: 26923269]
- [27]. Hayashida S, Arimoto A, Kuramoto Y, et al. (2010) Fasting promotes the expression of SIRT1, an NAD⁺-dependent protein deacetylase, via activation of PPAR α in mice. *Mol Cell Biochem* 339(1–2): 285–292. 10.1007/s11010-010-0391-z [PubMed: 20148352]
- [28]. Lee SH, Lee JH, Lee HY, Min KJ (2019) Sirtuin signaling in cellular senescence and aging. *BMB Rep* 52(1): 24–34 [PubMed: 30526767]
- [29]. Kobayashi K, Forte TM, Taniguchi S, Ishida BY, Oka K, Chan L (2000) The *db/db* mouse, a model for diabetic dyslipidemia: molecular characterization and effects of Western diet feeding. *Metabolism* 49(1): 22–31. 10.1016/s0026-0495(00)90588-2 [PubMed: 10647060]
- [30]. Antonetti DA, Barber AJ, Khin S, Lieth E, Tarbell JM, Gardner TW (1998) Vascular permeability in experimental diabetes is associated with reduced endothelial occludin content: vascular endothelial growth factor decreases occludin in retinal endothelial cells. *Penn State Retina Research Group. Diabetes* 47(12): 1953–1959. 10.2337/diabetes.47.12.1953 [PubMed: 9836530]
- [31]. Stewart EA, Samaranyake GJ, Browning AC, Hopkinson A, Amoaku WM (2011) Comparison of choroidal and retinal endothelial cells: characteristics and response to VEGF isoforms and anti-VEGF treatments. *Exp Eye Res* 93(5): 761–766. 10.1016/j.exer.2011.09.010 [PubMed: 21970900]
- [32]. Antonetti DA, Wolpert EB, DeMaio L, Harhaj NS, Scaduto RC Jr. (2002) Hydrocortisone decreases retinal endothelial cell water and solute flux coincident with increased content and decreased phosphorylation of occludin. *J Neurochem* 80(4): 667–677. 10.1046/j.0022-3042.2001.00740.x [PubMed: 11841574]
- [33]. Gardner TW, Leshner T, Khin S, Vu C, Barber AJ, Brennan WA Jr. (1996) Histamine reduces ZO-1 tight-junction protein expression in cultured retinal microvascular endothelial cells. *Biochem J* 320 (Pt 3): 717–721. 10.1042/bj3200717 [PubMed: 9003354]
- [34]. Strober W (2015) Trypan Blue Exclusion Test of Cell Viability. *Curr Protoc Immunol* 111: A3.B.1–A3.B.3. 10.1002/0471142735.ima03bs111 [PubMed: 26529666]
- [35]. Saadane A, Mast N, Trichonas G, et al. (2019) Retinal Vascular Abnormalities and Microglia Activation in Mice with Deficiency in Cytochrome P450 46A1-Mediated Cholesterol Removal. *Am J Pathol* 189(2): 405–425. 10.1016/j.ajpath.2018.10.013 [PubMed: 30448403]
- [36]. Hernandez C, Burgos R, Canton A, Garcia-Arumi J, Segura RM, Simo R (2001) Vitreous levels of vascular cell adhesion molecule and vascular endothelial growth factor in patients with proliferative diabetic retinopathy: a case-control study. *Diabetes Care* 24(3): 516–521. 10.2337/diacare.24.3.516 [PubMed: 11289478]
- [37]. Capozzi ME, Hammer SS, McCollum GW, Penn JS (2016) Epoxygenated Fatty Acids Inhibit Retinal Vascular Inflammation. *Sci Rep* 6: 39211. 10.1038/srep39211 [PubMed: 27966642]
- [38]. Levitsky Y, Pegouske DJ, Hammer SS et al. (2019) Micro-Respirometry of Whole Cells and Isolated Mitochondria. *RSC Advances* 9(57):33257–33267. doi: 10.1039/c9ra05289e [PubMed: 32123561]
- [39]. Lydic TA, Busik JV, Reid GE (2014) A monophasic extraction strategy for the simultaneous lipidome analysis of polar and nonpolar retina lipids. *J Lipid Res* 55(8): 1797–1809. 10.1194/jlr.D050302 [PubMed: 24879804]
- [40]. McDonald JG, Thompson BM, McCrum EC, Russell DW (2007) Extraction and analysis of sterols in biological matrices by high performance liquid chromatography electrospray ionization mass spectrometry. *Methods Enzymol* 432: 145–170. 10.1016/S0076-6879(07)32006-5 [PubMed: 17954216]

- [41]. Machacek M, Saunders H, Zhang Z, et al. (2019) Elevated O-GlcNAcylation enhances proinflammatory Th17 function by altering the intracellular lipid microenvironment. *J Biol Chem* 294(22): 8973–8990. 10.1074/jbc.RA119.008373 [PubMed: 31010828]
- [42]. Beli E, Yan Y, Moldovan L, et al. (2018) Restructuring of the Gut Microbiome by Intermittent Fasting Prevents Retinopathy and Prolongs Survival in *db/db* Mice. *Diabetes* 67(9): 1867–1879. 10.2337/db18-0158 [PubMed: 29712667]
- [43]. Asare-Bediako B, Noothi SK, Li Calzi S, et al. (2020) Characterizing the Retinal Phenotype in the High-Fat Diet and Western Diet Mouse Models of Prediabetes. *Cells* 9(2). 10.3390/cells9020464
- [44]. Prusky GT, Alam NM, Beekman S, Douglas RM (2004) Rapid quantification of adult and developing mouse spatial vision using a virtual optomotor system. *Invest Ophthalmol Vis Sci* 45(12): 4611–4616. 10.1167/iovs.04-0541 [PubMed: 15557474]
- [45]. Qi X, Pay SL, Yan Y, et al. (2017) Systemic Injection of RPE65-Programmed Bone Marrow-Derived Cells Prevents Progression of Chronic Retinal Degeneration. *Mol Ther* 25(4): 917–927. 10.1016/j.ymthe.2017.01.015 [PubMed: 28202390]
- [46]. Hazra S, Jarajapu YP, Stepps V, et al. (2013) Long-term type 1 diabetes influences haematopoietic stem cells by reducing vascular repair potential and increasing inflammatory monocyte generation in a murine model. *Diabetologia* 56(3): 644–653. 10.1007/s00125-012-2781-0 [PubMed: 23192694]
- [47]. Vieira CP, Fortmann SD, Hossain M, et al. (2020) Selective LXR agonist DMHCA corrects retinal and bone marrow dysfunction in type 2 diabetes. *JCI Insight* 5(13). 10.1172/jci.insight.137230
- [48]. Horne BD, Grajower MM, Anderson JL (2020) Limited Evidence for the Health Effects and Safety of Intermittent Fasting Among Patients With Type 2 Diabetes. *JAMA* 10.1001/jama.2020.3908
- [49]. Li C, Sadraie B, Steckhan N, et al. (2017) Effects of A One-week Fasting Therapy in Patients with Type-2 Diabetes Mellitus and Metabolic Syndrome - A Randomized Controlled Explorative Study. *Exp Clin Endocrinol Diabetes* 125(9): 618–624. 10.1055/s-0043-101700 [PubMed: 28407662]
- [50]. Dimmeler S, Zeiher AM (2004) Vascular repair by circulating endothelial progenitor cells: the missing link in atherosclerosis? *J Mol Med (Berl)* 82(10): 671–677. 10.1007/s00109-004-0580-x [PubMed: 15322703]
- [51]. Jarajapu YP, Hazra S, Segal M, et al. (2014) Vasoreparative dysfunction of CD34+ cells in diabetic individuals involves hypoxic desensitization and impaired autocrine/paracrine mechanisms. *PLoS One* 9(4): e93965. 10.1371/journal.pone.0093965 [PubMed: 24713821]
- [52]. Fadini GP, de Kreutzenberg S, Agostini C, et al. (2009) Low CD34+ cell count and metabolic syndrome synergistically increase the risk of adverse outcomes. *Atherosclerosis* 207(1): 213–219. 10.1016/j.atherosclerosis.2009.03.040 [PubMed: 19406403]
- [53]. Tikhonenko M, Lydic TA, Opreanu M, et al. (2013) *n*-3 polyunsaturated fatty acids prevent diabetic retinopathy by inhibition of retinal vascular damage and enhanced endothelial progenitor cell reparative function. *PLoS One* 8(1): e55177. 10.1371/journal.pone.0055177 [PubMed: 23383097]
- [54]. Busik JV, Tikhonenko M, Bhatwadekar A, et al. (2009) Diabetic retinopathy is associated with bone marrow neuropathy and a depressed peripheral clock. *J Exp Med* 206(13): 2897–2906. 10.1084/jem.20090889 [PubMed: 19934019]
- [55]. Balestrieri ML, Servillo L, Esposito A, et al. (2013) Poor glycaemic control in type 2 diabetes patients reduces endothelial progenitor cell number by influencing SIRT1 signalling via platelet-activating factor receptor activation. *Diabetologia* 56(1): 162–172. 10.1007/s00125-012-2749-0 [PubMed: 23070058]
- [56]. Lemarie CA, Shbat L, Marchesi C, et al. (2011) Mthfr deficiency induces endothelial progenitor cell senescence via uncoupling of eNOS and downregulation of SIRT1. *Am J Physiol Heart Circ Physiol* 300(3): H745–753. 10.1152/ajpheart.00321.2010 [PubMed: 21169404]

- [57]. Yuen DA, Zhang Y, Thai K, et al. (2012) Angiogenic dysfunction in bone marrow-derived early outgrowth cells from diabetic animals is attenuated by SIRT1 activation. *Stem cells translational medicine* 1(12): 921–926. 10.5966/sctm.2012-0026 [PubMed: 23283553]
- [58]. Sene A, Apte RS (2014) Eyeballing cholesterol efflux and macrophage function in disease pathogenesis. *Trends Endocrinol Metab* 25(3): 107–114. 10.1016/j.tem.2013.10.007 [PubMed: 24252662]
- [59]. Guo W, Zhou Q, Jia Y, Xu J (2019) Increased Levels of Glycated Hemoglobin A1c and Iron Deficiency Anemia: A Review. *Med Sci Monit* 25: 8371–8378. 10.12659/MSM.916719 [PubMed: 31696865]
- [60]. Minor RK, Baur JA, Gomes AP, et al. (2011) SRT1720 improves survival and healthspan of obese mice. *Sci Rep* 1: 70. 10.1038/srep00070 [PubMed: 22355589]
- [61]. Mitchell SJ, Martin-Montalvo A, Mercken EM, et al. (2014) The SIRT1 activator SRT1720 extends lifespan and improves health of mice fed a standard diet. *Cell Rep* 6(5): 836–843. 10.1016/j.celrep.2014.01.031 [PubMed: 24582957]
- [62]. Milne JC, Lambert PD, Schenk S, et al. (2007) Small molecule activators of SIRT1 as therapeutics for the treatment of type 2 diabetes. *Nature* 450(7170): 712–716. 10.1038/nature06261 [PubMed: 18046409]
- [63]. Pacholec M, Bleasdale JE, Chrnyk B, et al. (2010) SRT1720, SRT2183, SRT1460, and resveratrol are not direct activators of SIRT1. *J Biol Chem* 285(11): 8340–8351. 10.1074/jbc.M109.088682 [PubMed: 20061378]
- [64]. Zarse K, Schmeisser S, Birringer M, Falk E, Schmoll D, Ristow M (2010) Differential effects of resveratrol and SRT1720 on lifespan of adult *Caenorhabditis elegans*. *Horm Metab Res* 42(12): 837–839. 10.1055/s-0030-1265225 [PubMed: 20925017]
- [65]. Belden WJ, Dunlap JC (2008) SIRT1 is a circadian deacetylase for core clock components. *Cell* 134(2): 212–214. 10.1016/j.cell.2008.07.010 [PubMed: 18662537]
- [66]. Antoni R, Johnston KL, Collins AL, Robertson MD (2017) Effects of intermittent fasting on glucose and lipid metabolism. *Proc Nutr Soc* 76(3): 361–368. 10.1017/S0029665116002986 [PubMed: 28091348]
- [67]. Mattson MP, Longo VD, Harvie M (2017) Impact of intermittent fasting on health and disease processes. *Ageing Res Rev* 39: 46–58. 10.1016/j.arr.2016.10.005 [PubMed: 27810402]
- [68]. Kraus WE, Bhapkar M, Huffman KM, et al. (2019) 2 years of calorie restriction and cardiometabolic risk (CALERIE): exploratory outcomes of a multicentre, phase 2, randomised controlled trial. *Lancet Diabetes Endocrinol* 7(9): 673–683. 10.1016/S2213-8587(19)30151-2 [PubMed: 31303390]
- [69]. Mishra M, Flaga J, Kowluru RA (2016) Molecular Mechanism of Transcriptional Regulation of Matrix Metalloproteinase-9 in Diabetic Retinopathy. *J Cell Physiol* 231(8): 1709–1718. 10.1002/jcp.25268 [PubMed: 26599598]

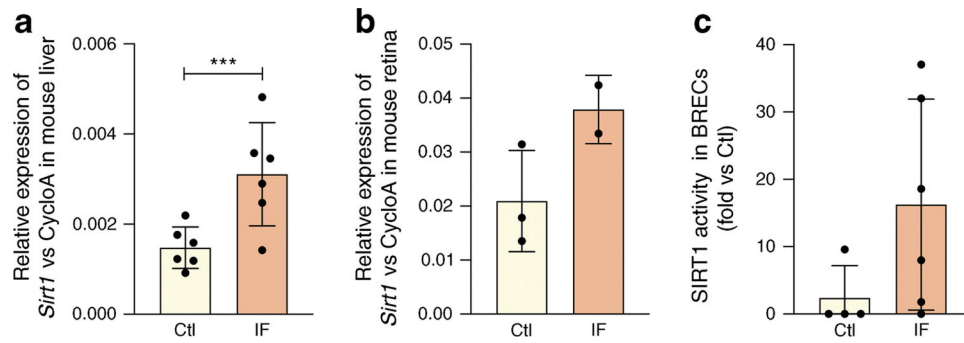


Fig. 1.

Fasting increases *Sirt1* expression and activity. (a) Liver and (b) retinal *Sirt1* mRNA expression is increased by IF in mice (48 h fast) when compared with non-fasting controls. (c) IF increases SIRT1 HDAC activity in mouse retinal tissue when compared with non-fasting controls, *** $p < 0.001$. Data are represented as mean \pm SEM. Ctl, control; CycloA, cyclophilin A; F355/F460, fluorescence at 355/460 nm

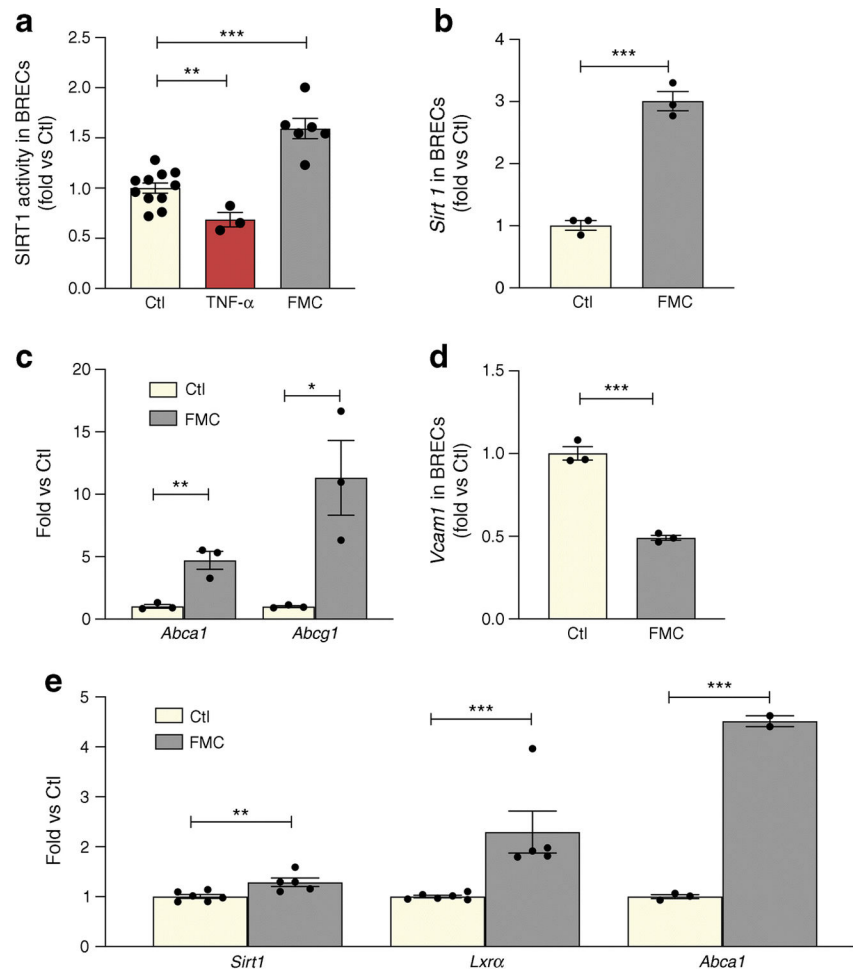


Fig. 2. FMC activates the SIRT1/LXR signalling pathway in BRECs and neuronal (R28) cells. FMC (0% FBS, 24 h) in BRECs activates (a) SIRT1 HDAC activity, with TNF- α used as a positive control, (b) *Sirt1* mRNA expression, and (c) increased expression of RCT genes (*Abca1* and *Abcg1*). (d) *Vcam1* is decreased after treatment with FMC conditions. (e) Treatment of R28 cells with FMC increases expression of *Sirt1* and *Lxra* mRNA, as well as LXR α activity, as measured by *Abca1* mRNA expression * $p < 0.05$, ** $p < 0.01$, *** $p < 0.001$. Data are represented as mean \pm SEM. Ctl, control

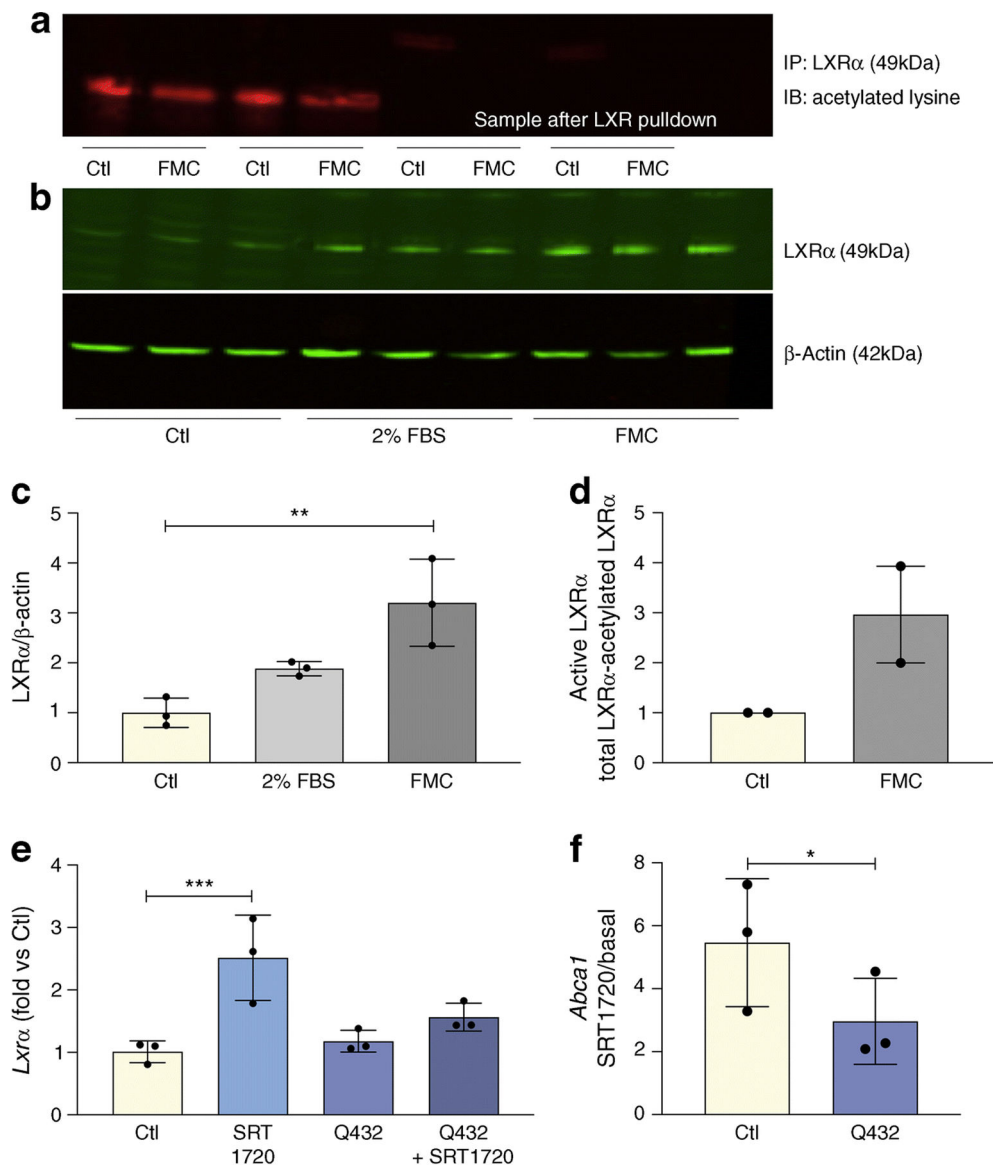
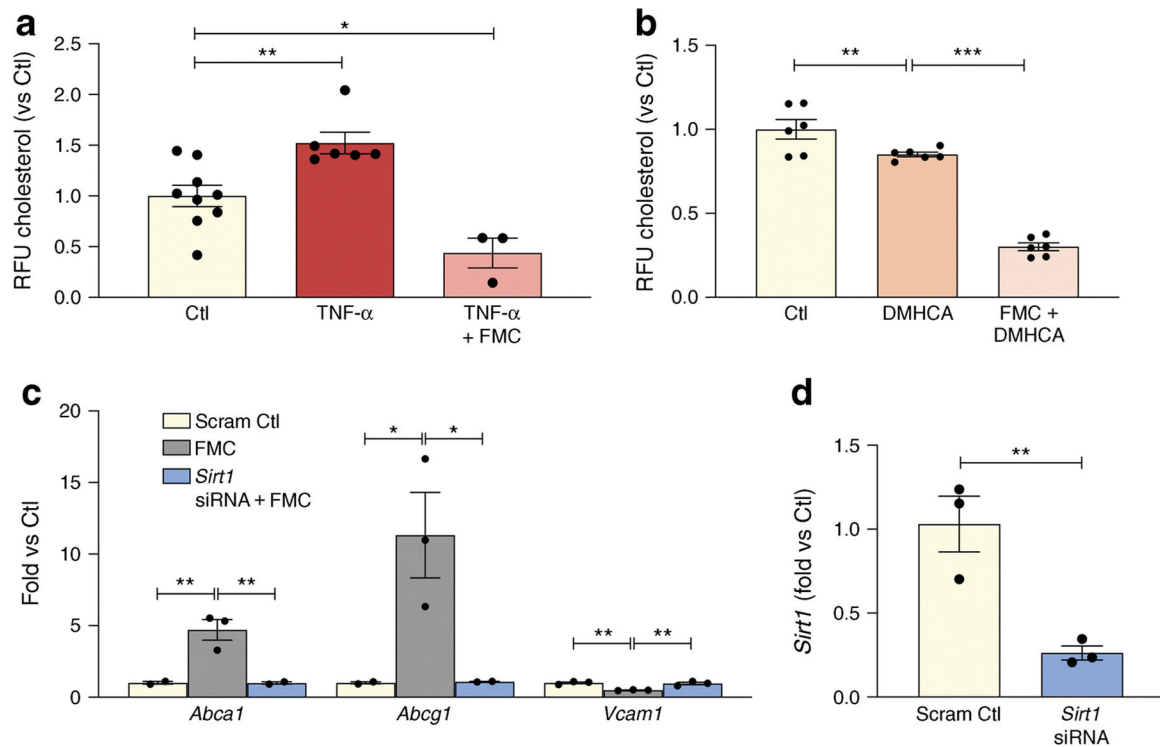


Fig. 3. FMC increases LXR α activity via deacetylation. FMC (0% FBS, 24 h) in BRECs (a) decreases levels of non-active, deacetylated LXR α ; and (b) increases total LXR α protein levels, quantification shown in (c). The data for active LXR quantified by subtracting acetylated LXR α in (a) from total LXR α in (b) is presented in (d) as mean \pm SEM. BRECs were treated with SRT1720 (1 μ mol/l) and/or infected with constitutively acetylated LXR α (Q432) for 24 h. Expression of *Lxr α* (e) or SIRT1-dependent activation of LXR α (f) presented as SRT1720-induced increase in *Abca1* expression in BRECs (Ctl) and BRECs infected with Q432. Ratios determined from three independent experiments, * p <0.05, ** p <0.01, *** p <0.001. Data are represented as mean \pm SEM. Ctl, control; IB, immunoblot; IP, immunoprecipitation

**Fig. 4.**

SIRT1 plays an important role in fasting mediated decrease of cholesterol levels in BRECs. (a) TNF- α treatment causes a significant increase in cholesterol levels while FMC (0% FBS, 24 h) prevents this TNF- α -induced increase. (b) This decrease is amplified by administration of the LXRA activator, DMHCA. (c) SIRT1 was reduced by exposure of the BRECs to *Sirt1* siRNA. Administration of *Sirt1* siRNA prevented serum-induced upregulation of *Abca1* and *Abcg1* and inhibited the downregulation of the proinflammatory gene, *Vcam1*. (d) *Sirt1* knockdown efficiency. * $p < 0.05$, ** $p < 0.01$, *** $p < 0.001$. Data are represented as mean \pm SEM. Ctl, control; CycloA, cyclophilin A, Scram Ctl; scrambled *Sirt1* siRNA sequence used in 4c and 4d

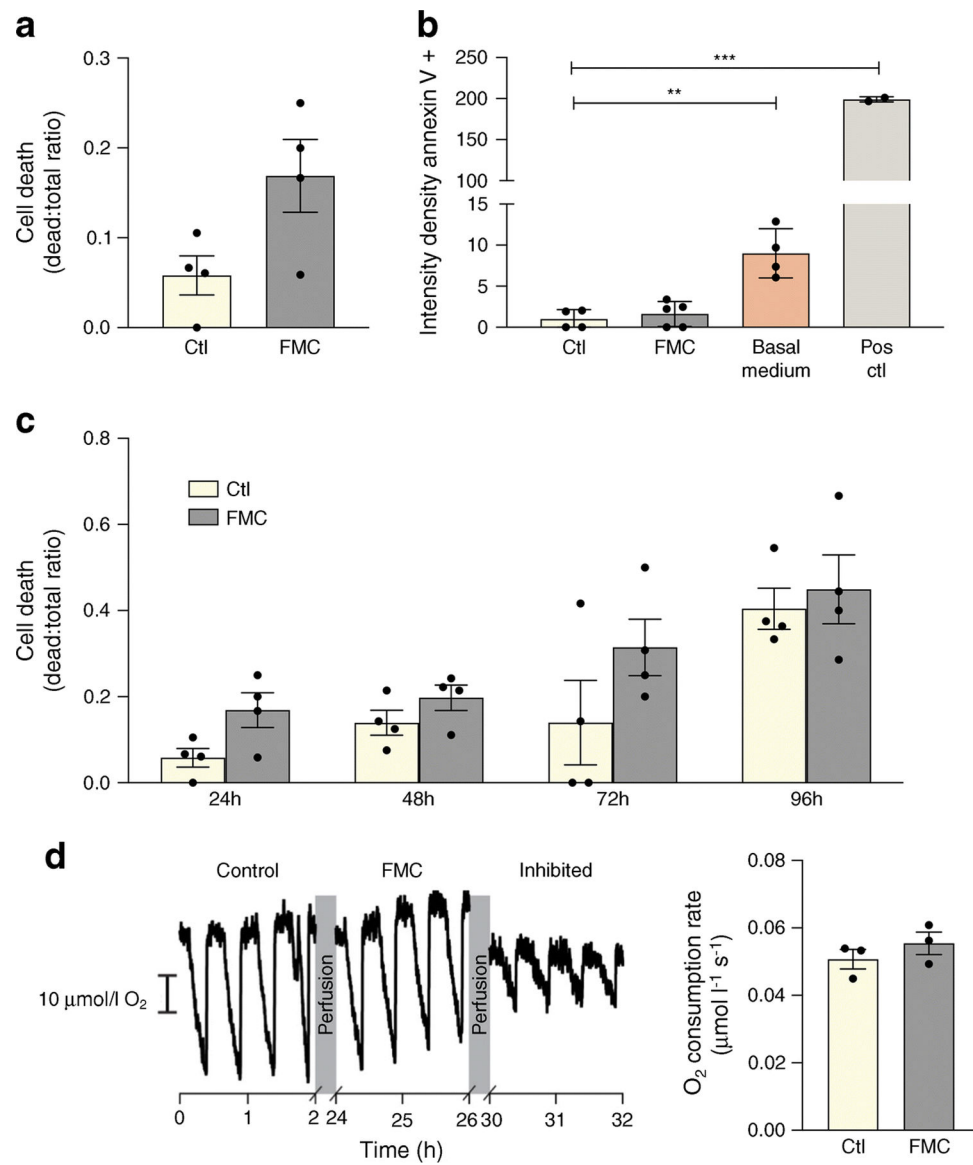


Fig. 5. FMC does not significantly impact cell death or mitochondrial substrate-supported respiration in BRECs. **(a, b)** FMC (0% FBS, 24 h) does not significantly increase cell death. Basal media is comprised of only MCB131 media without the addition of growth factors or supplements (m8537). Positive control (Pos ctl): 50°C for 10 min. **(c)** Time course of cell death assay. **(d)** Respiratory activity of BRECs cultured in control or FMC media after 24 h, ** $p < 0.01$, *** $p < 0.001$, Data are represented as mean \pm SEM. Scale bar, 10 $\mu\text{mol/l O}_2$. Ctl, control

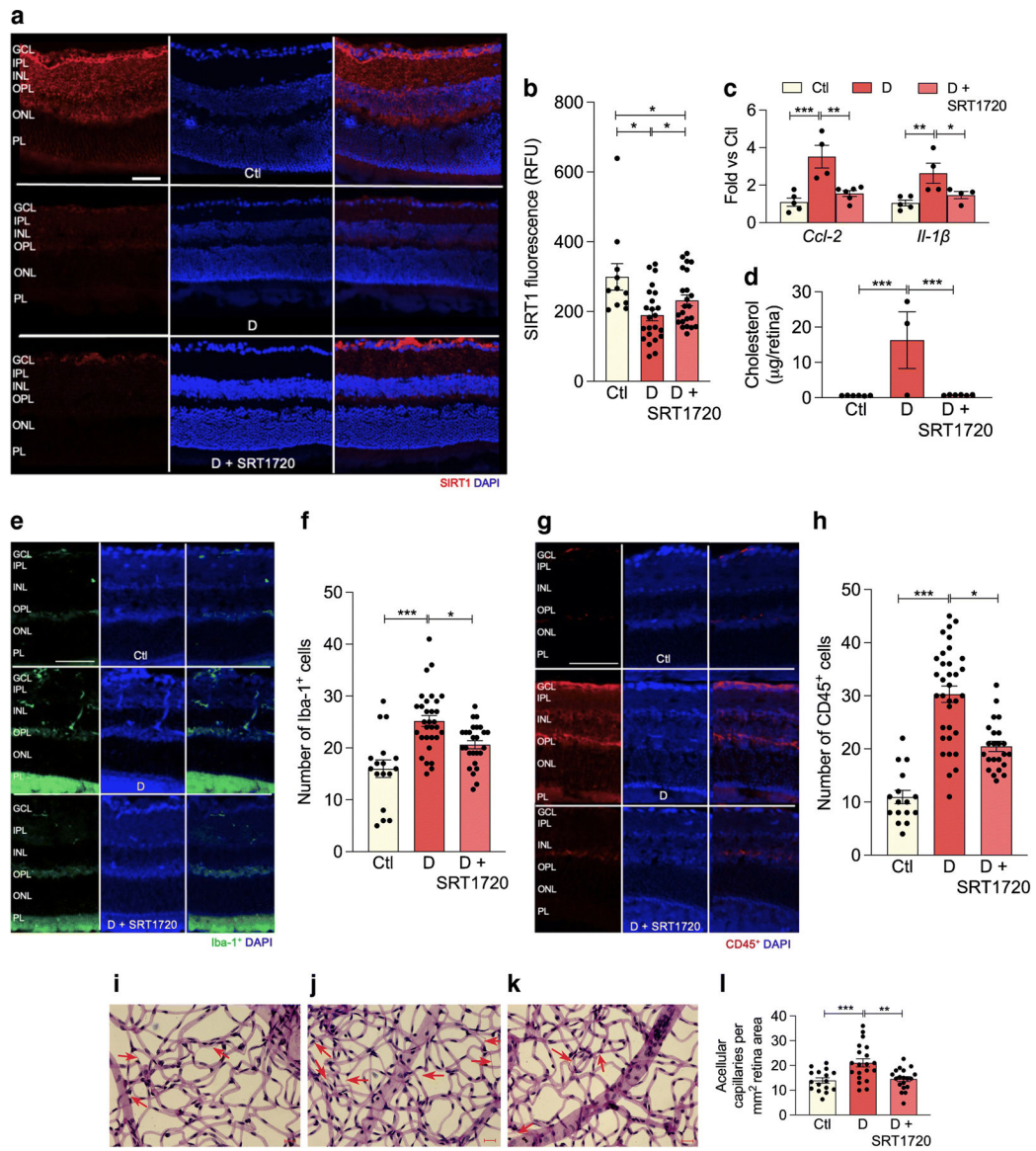


Fig. 6. SRT1720 increases SIRT1 expression in retina of *db/db* mice with 6 month duration of diabetes. **(a)** Retinal sections from non-diabetic controls (top), diabetic mice fed normal chow (middle) or chow containing SRT1720 (bottom) were stained with anti-SIRT1 antibody (red) and DAPI was used to stain nuclei (blue). Quantification is shown in **(b)**; several replicate samples were stained from $n=4$ mice. **(c, d)** Diabetes significantly increases proinflammatory markers *Ccl-2*, *Il-1β* mRNA expression **(c)** and significantly increases retinal cholesterol levels (mass spectrometry analysis) **(d)**; the SIRT1 agonist SRT1720 restores *Ccl-2* and *Il-1β* **(c)** and cholesterol **(d)**, to non-diabetic levels; $n=4-5$ mice. **(e-h)** Diabetes increases, while SRT1720 normalises, the cell number of Iba-1⁺ **(e, f)** and CD45⁺ **(g, h)** cells in the retina, $n=5$ from 3 to 5 sections at 100 μm interval for each eye with a minimum of four images for section. **(i-l)** Acellular capillary formation (red arrows) was examined in non-diabetic animals **(i)**, and in diabetic animals fed control chow **(j)** or chow

containing SRT1720 (**k**). Diabetes significantly increases acellular capillary formation (**j**) while administration of the SIRT1 agonist prevents diabetes-induced acellular capillary formation (**k**). Quantification is shown in (**i**); $n=5$ from 4 to 5 images per mm^2 retina area; * $p<0.05$, ** $p<0.01$, *** $p<0.001$. Data are represented as mean \pm SEM. Scale bars, 20 μm . Ctl, control (*db/m*); D, diabetic (*db/db*); GCL, ganglion cell layer; INL, inner nuclear layer; IPL, inner plexiform layer; ONL, outer nuclear layer; OPL, outer plexiform layer; PL, photoreceptor layer. RFU, relative fluorescence units

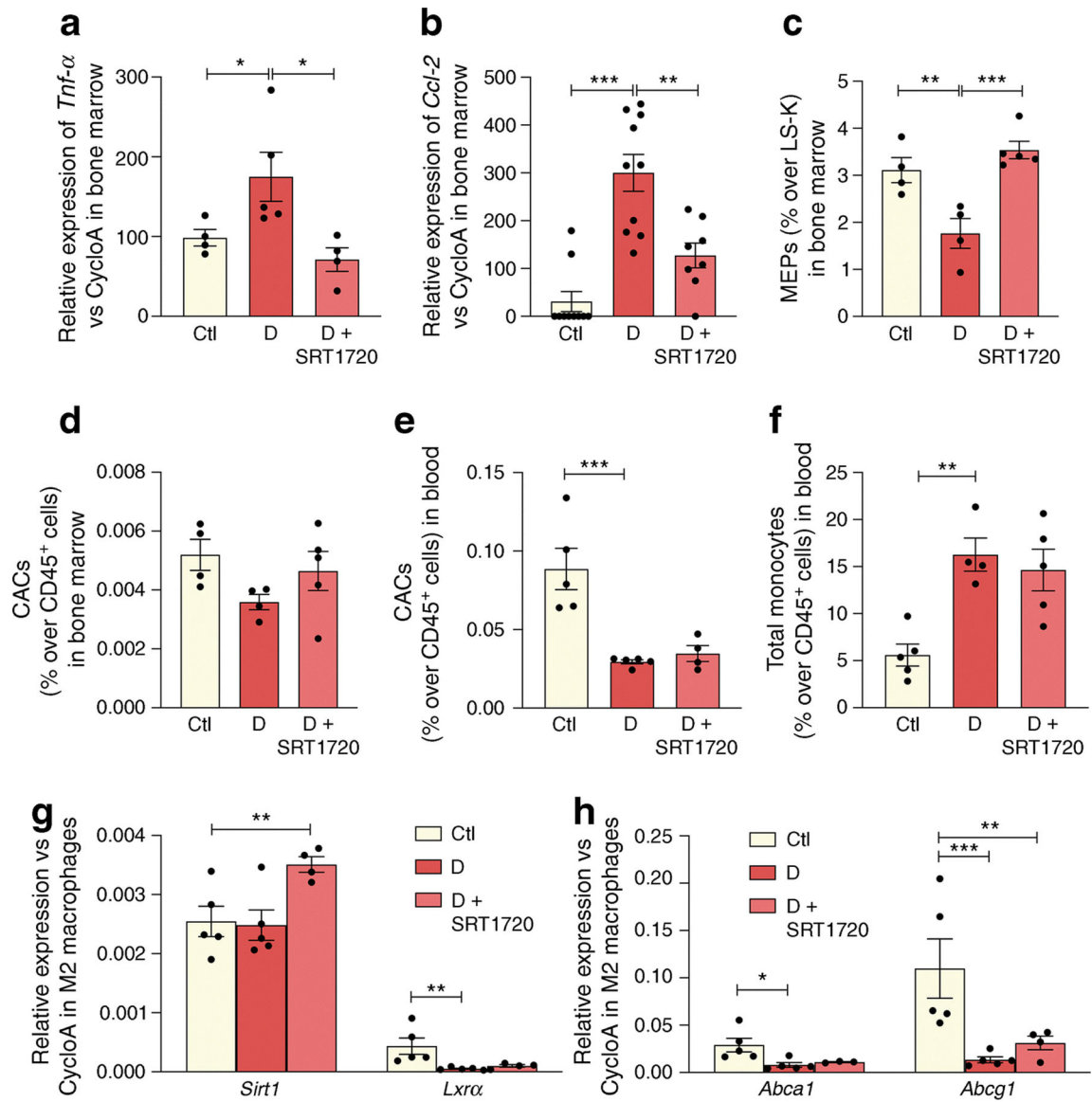


Fig. 7. SRT1720 normalises inflammatory and reparative cell damage in the bone marrow and blood of *db/db* mice with 6 month duration of diabetes. **(a, b)** *Tnf- α* ($n=4-5$ mice) **(a)** and *Ccl-2* ($n=5$ mice carried out in duplicate) **(b)** expression in the bone marrow of non-diabetic controls, and diabetic mice fed normal chow or chow containing SRT1720. **(c, d)** Diabetes significantly decreases the number of MEPS **(c)** and CACs **(d)** in the bone marrow, while SRT1720 restores MEP to non-diabetic levels, $n=4-5$. **(e, f)** In the blood, diabetes significantly decreases the number of reparative CACs **(e)** and increases the number of inflammatory circulating total monocytes **(f)**; $n=4-5$. **(g, h)** In M2 macrophages, diabetes induces decrease in the expression of *Lxra* and LXR-controlled target genes (*Abca1* and *Abcg1*). SRT1720 increases *Sirt1* expression in M2 macrophages **(g)**, leading to upregulation of LXR activity as shown by an increase in *Abcg1* expression **(h)**; $n=4-5$;

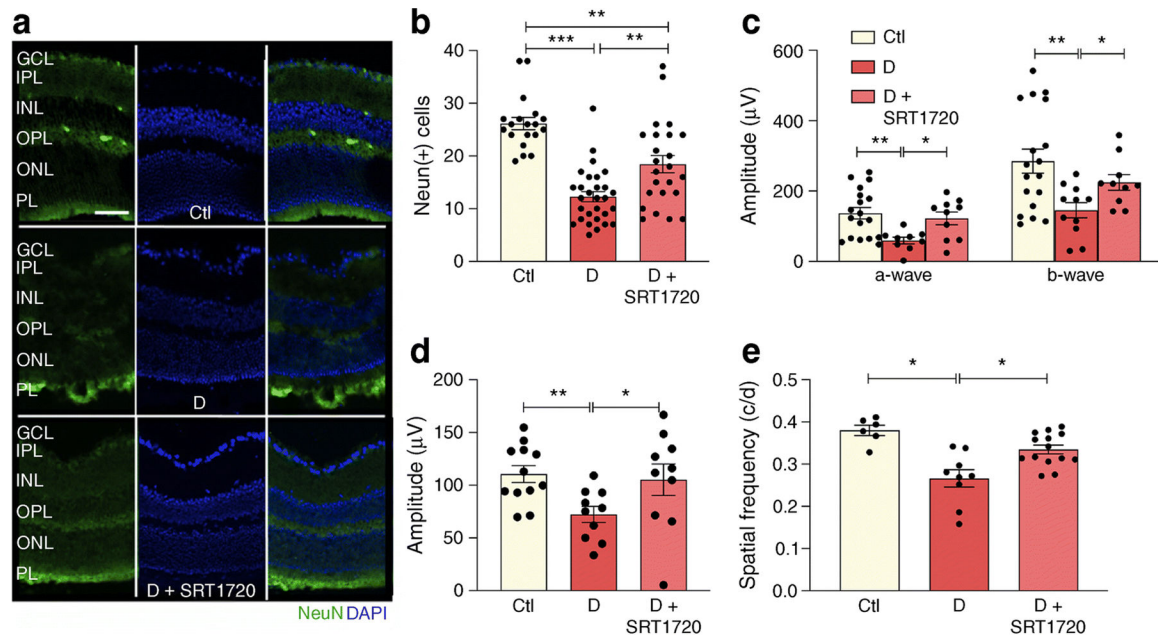
* $p < 0.05$, ** $p < 0.01$, *** $p < 0.001$. Data are represented as mean \pm SEM. Ctl, control (*db/m*); CycloA, cyclophilin A; D, diabetic (*db/db*); LS-K, Lin⁻Sca⁻Kit⁺

Author Manuscript

Author Manuscript

Author Manuscript

Author Manuscript

**Fig. 8.**

SRT1720 prevents diabetes-induced NeuN⁺ retinal decrease and improves visual and OKN response in *db/db* mice. **(a, b)** Chronic diabetes is associated with neuronal loss in the retina as demonstrated by reduced NeuN⁺ expression (green) in *db/db* mice when compared with non-diabetic *db/m* controls **(a)**. Pharmacological SIRT1 activation using STR1720 in diabetic mice partly restores NeuN⁺ expression to control levels **(a)**. Quantification shown in **(b)**; $n=4$ from 3–5 sections at 100 μ m interval for each eye with a minimum of four images per section; NeuN⁺ cells were quantified only in the GCL. **(c)** Analysis of the ERG showed diabetes-induced reduction of scotopic a- and b-waves; an increase and improvement in scotopic a- and b-wave was observed in diabetic mice treated with SRT1720 compared with diabetic mice on control chow. **(d)** An improvement in photopic b-wave was observed in diabetic mice treated with SRT1720 compared with diabetic mice on control chow; $n=5-6$ carried out from right and left eyes. **(e)** In diabetic mice, the OKN response is reduced compared with age-matched non-diabetic control mice. Diabetic mice treated with SRT1720 showed an improvement in visual acuity compared with diabetic mice on control chow; $n=4-6$ carried out from right and left eyes; * $p<0.05$, ** $p<0.01$ *** $p<0.001$. Data are represented as mean \pm SEM. Scale bar, 50 μ m. Ctl, control (*db/m*); D, diabetic (*db/db*); GCL, ganglion cell layer; INL, inner nuclear layer; IPL, inner plexiform layer; ONL, outer nuclear layer; OPL, outer plexiform layer; PL, photoreceptor layer

Table 1.

Primer sequences

Species	Name	Forward (5' to 3')	Reverse (5' to 3')	Accession ID
Bovine	SIRT1	CCC TGA AAG TAA GAC CAG TAG C	GTG AGG CAA AGG TTC CCT ATT A	NM_001192980.3
	ABCA1	CTC AGT GGG ATG GAT GGT AAA G	TGG CAA TCA GCA GTC TCT TC	NM_001024693.1
	ABCG1	AGA CCT GCC ATT TCC AGA AG	GAT GAG ACG CAG GGA GAT AAA G	NM_001205528.3
	VCAM1	TGCAGGGTTCCTAATGT GTATC	GTAAGAAAGCCCTAGAG ACCAAG	NM_174484.1
	Cyclophilin A	GAGCACTGGAGAGAAA GGATTT	GACTTGCCACCAGTACC ATTAT	NM_178320.2
Rat (used For R28 cell culture studies)	SIRT1	CATAGGTTAGGTGGCG AGTATG	GTTGGTGGCAACTCTGA TAAATG	NM_001372090.1
	ABCA1	TTGGATTCGGCTGTGAG TATTT	GGACTGAGGTGGTAA GATTG	NM_178095.2
	LXR α	TGGCACTAAAGAGAGTC AAAGG	GGCTCTCCTGGCTAGTT TATTT	NM_031627.2
	Cyclophilin A	TGGCAAGACCAGCAAG AA	CTCCTGAGCTACAGAAG GAATG	NM_017101.1